ELSEVIER

Sensors and Actuators B 62 (2000) 121–130

SENSORS AND ACTUATORS B CHEMICAL

www.elsevier.nl/locate/sensorb

Vapor recognition with an integrated array of polymer-coated flexural plate wave sensors

Qing-Yun Cai [a], Jeongim Park [a], Dylan Heldsinger [a], Meng-Da Hsieh [a], Edward T. Zellers [a,b,*]

[a] *Department of Environmental Health Sciences, University of Michigan, Ann Arbor, MI 48109-2029, USA*
[b] *Department of Chemistry, University of Michigan, Ann Arbor, MI 48109-2029, USA*

Received 23 July 1999; received in revised form 24 September 1999; accepted 24 September 1999

Abstract

Preliminary testing of a prototype instrument employing an integrated array of six polymer-coated flexural plate wave (FPW) sensors and an adsorbent preconcentrator is described. Responses to thermally desorbed samples of individual organic solvent vapors and binary and ternary vapor mixtures are linear with concentration, and mixture responses are equivalent to the sums of the responses of the component vapors, which co-elute from the preconcentrator in most cases. Limits of detection as low as 0.3 ppm are achieved from a 60-s (34 cm^3) air sample and peak widths at half-maximum range from 1 to 4 s. Tests at different flow rates suggest that the kinetics of vapor sorption in the sensor coating films may limit responses at higher flow rates, however, low data acquisition rates may also be contributory. Assessments of array performance using independent test data and Monte Carlo simulations with pattern recognition indicate that individual vapors and certain binary and ternary mixtures can be recognized/discriminated with very low error. More complex mixtures, and those containing homologous vapors, are problematic. This is the first report demonstrating multi-vapor analysis with an integrated FPW sensor array.

Keywords: Vapor sensor; Sensor array; Acoustic-wave sensor; Pattern recognition; Vapor recognition; Flexural plate wave

1. Introduction

Arrays of partially selective sensors of various types have been used to analyze multiple individual vapors and simple vapor mixtures [1–10]. In most cases, the sensors in the array are overlaid with interfacial films consisting of polymers of diverse structures into which vapors rapidly and reversibly partition to varying degrees. The differential partitioning gives rise to the characteristic response patterns used for vapor recognition.

Where measurement of low concentrations of organic vapors in the ambient environment are required, preconcentration via a bed of a hydrophobic granular porous polymer can be useful. In addition to increasing sensitivity and reducing limits of detection (LOD), preconcentration can provide immunity from baseline drift as well as a degree of water-vapor compensation [2,11,12].

The prototype instrument described here employs an array of flexural plate wave (FPW) sensors, which are similar in many respects to the more common surface acoustic wave (SAW) sensors [1–4,13–18]. In both sensors, radio-frequency mechanical (acoustic) waves are generated within a piezoelectric substrate that has been coated with a chemically sensitive (e.g., polymer) film. The acoustic waves are launched and received by a pair of interdigital transducers (IDTs) on the device surface, and a feedback amplifier connecting the IDTs permits sustained oscillation at a frequency determined by the device structure. Small changes in the mass or viscoelastic properties of the coating film caused by interactions with gases or vapors result in a change of the acoustic wave velocity, which can be measured indirectly as a change in wave frequency using digital frequency counting electronics.

In contrast to the SAW device, the active region on which the acoustic waves travel in the FPW device is a membrane whose thickness is much smaller than the acoustic wavelength [13–18]. As a result, wave energy is

* Corresponding author. Department of Environmental Health Sciences, University of Michigan, 109 S. Observatory St., Ann Arbor, MI 48109-2029, USA. Tel.: +1-734-936-0766; fax: +1-734-763-8095; e-mail: ezellers@umich.edu

0925-4005/00/$ - see front matter
PII: S0925-4005(99)00381-0

present at both the front- and back-side of the membrane and the entire membrane undergoes mechanical flexure. For chemical sensing the polymer-coated FPW device has several potential advantages over SAW and thickness shear mode (TSM) sensors. These include: higher inherent mass sensitivity and lower operating frequency, which should lead to lower LODs; the capability to support thicker polymer layers without loss of oscillation, which should increase sensitivity; environmental isolation of the IDT electrodes by coating and exposing only the backside of the device membrane; and silicon-based fabrication, which permits reproducible production of integrated sensor arrays having a low total dead-volume. The latter becomes increasingly important in microanalytical systems employing smaller sample sizes and lower system flow rates [19]. Although individual polymer-coated FPW vapor sensors have been reported [15–18], there has yet to be a report of vapor sensing with an integrated array of FPW sensors.

In this article, preliminary testing of an instrument employing an integrated array of six FPW sensors and an upstream adsorbent preconcentrator is described. The basic operating features of the instrument are discussed and the effects on sensor responses of varying the sample volume and the sampling and desorption flow rates are assessed. Calibrated responses to several organic solvent vapors, individually and in simple mixtures, were used to establish LODs and sensitivities, and to provide a training set for pattern recognition analysis. Independent test data and Monte Carlo simulations were then used to evaluate the capability for vapor recognition and discrimination.

2. Experimental

2.1. Instrument description

The prototype instrument ($23 \times 23 \times 5$ cm) operates on AC power and contains the FPW sensor array, a capillary adsorbent preconcentrator with a resistive heater for thermal desorption, a diaphragm sampling pump (Model SP-550EC; Schwarzer Prazision, Essen, Germany), and control and drive electronics. A 30-cm^3 glass chamber connected just upstream of the pump dampens the pulsatory flow accompanying diaphragm displacement. A laptop computer coordinates the system operation, and processes and displays the sensor outputs in near real time. For this study, a manual, low-dead-volume, three-way valve (Model No. 86727; Hamilton, Reno, NV) was affixed to the inlet of the instrument to facilitate switching between vapor test-atmospheres and clean, dry air. The instrument and data acquisition software were developed by Berkeley MicroInstruments (Richmond, CA).

Each FPW device membrane is a layered composite, 5 μm thick, consisting of a silicon nitride layer (3 μm), a polished layer of p-doped polysilicon (0.5 μm), and a ZnO piezoelectric layer (1.5 μm) attached peripherally to the silicon substrate (Fig. 1). The IDTs comprise 25 pairs of Al electrodes, 0.3 μm thick, each patterned to a width of 20 μm and separated from adjacent electrodes by 20 μm to give an acoustic wavelength of 80 μm and a resonant frequency of 8 MHz. The input and output IDTs are separated by a gap of about 2 mm. Insertion losses for these devices are in the range of 30–40 dB.

The six FPW devices are integrated on a single chip measuring 9.5×12 mm and bonded into a hybrid integrated circuit (IC) package. Each device is driven at its self-resonant frequency at all times and connected sequentially to a feedback amplifier having a gain of 54 dB. Frequency measurements are mixed with a reference signal from a local oscillator (LO) generated by a direct digital synthesizer. The LO frequency is established at an initial value that is offset from those of the FPW devices by 30–150 kHz. The difference frequency from each sensor is divided by 255 and used to gate a 20-bit counter clocked at 25 MHz. Measurements from all six sensors in the array are collected every 120 ms. However, since the counting routine is nested within the control software program which also provides near-real-time data display and system monitoring functions, the effective frequency measurement rate is limited to a maximum of 2 Hz for the array.

A large aperture cut in the underside of the IC package exposes the backside of the FPW array membranes for interfacial coating application and vapor exposure testing, and the entire assembly is inverted so that the exposed membranes are facing upwards. The front side of the sensor array chip and the bond wires to the package are isolated from the environment. Vapors are delivered via a manifold machined to fit into the aperture in the package, forming a detector cell with a ~20-μl dead volume. The array package is heated to 30°C with a resistive heater on the manifold.

Fig. 2 shows a photograph of the mounted array (manifold removed). The shadowed regions are the trenches formed in the substrate when fabricating the membranes.

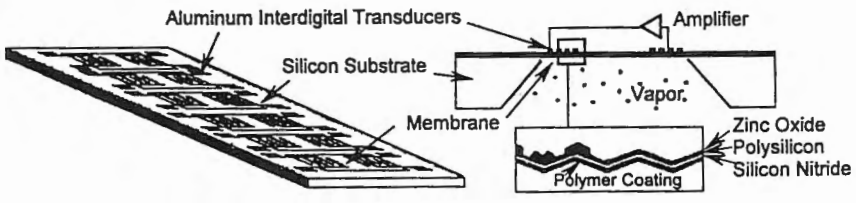

Fig. 1. Integrated FPW six-sensor array and structure of individual sensor.

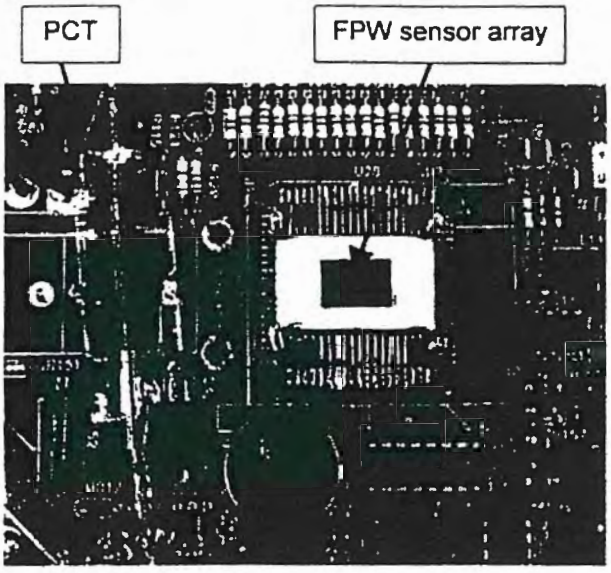

Fig. 2. Photograph showing the inverted sensor array and preconcentrator (PCT).

These measure approximately 1.2 × 8 mm and are 300 μm deep, giving an individual sensor-cell volume of about 3 μl.

The preconcentrator, also shown in Fig. 2, is a 200-μl glass capillary (0.1 cm i.d. × 7 cm length) packed with ~ 20 mg of 60/80 mesh Tenax-GR® granular adsorbent held in place with steel wool. A gold-wire resistive heater wrapped along the length of the capillary provides rapid heating and flash desorption of collected vapors. Preliminary testing established that a voltage of 6.8 V was required to reach and maintain a desorption temperature of ~ 200°C for 2 s, which was deemed adequate for efficient vapor desorption. The heater temperature was, therefore, not monitored in real-time.

The onboard diaphragm pump draws a sample through the preconcentrator and over the sensor array at an adjustable flow rate between 10 and 36 ml/min. The preconcentrator retains the incoming vapors as well as a fraction of the incoming water vapor from the matrix of air at 50% relative humidity used in all tests. After a predefined sampling period the preconcentrator is flash heated, the vapors are desorbed and distributed over the sensors in the array, and collection of the next sample begins. A typical analytical cycle requires a total of 70 s from the start of sample collection to elution of the analyte peaks. For this study, the maxima of the eluting peaks were used for quantification and response pattern generation. An external cartridge containing several grams of Drierite® provided a source of clean, dry air during periods when test atmosphere concentrations were being changed.

The control and display algorithms were written in the LabVIEW® graphical programming environment (Version 4.0.1; National Instruments, Austin, TX). The user sets most system parameters, including preconcentration time, desorption-heater pulse width and voltage, array temperature, and sensor data acquisition cycle. Displayed data include graphs of each FPW sensor frequency, array temperature, elapsed time, and preconcentrator status (on or off). The duration of the sample collection and desorption heating cycles are preset and the instrument proceeds through multiple cycles (typically four) automatically once a run is initiated. Collected response data are stored and subsequently treated with a spreadsheet package.

2.2. Coating selection and deposition

An initial set of polymer coatings spanning a broad range of functional groups was selected using linear solvation energy relationship (LSER) concepts [20–22] and results of previous studies of polymer-coated SAW sensors [1–3,11,22]. These included polyisobutylene (PIB), polyepichlorohydrin (PECH), polydiphenoxyphosphazene (PDPP), phenylmethyldiphenyl-silicone (OV-25), biscyanyoallyl polysiloxane (OV-275), and fluoropolyol (FPOL). PIB, PECH, and PDPP were obtained from Scientific Polymer Products (Ontario, NY). OV-25 and OV-275 were obtained from Supelco (Bellefonte, PA), and FPOL was obtained from Dr. A. Snow of the U.S. Naval Research Laboratory.

Each polymer was applied by airbrush as a solution (0.2%w/v) in chloroform (PIB, FPOL), toluene (PDPP, PECH), or acetone (OV-25, OV-275) while monitoring the sensor frequency. A mask fashioned from a surplus array whose membranes had been reamed out was used to confine the depositions to the individual sensors. Prior to deposition, the array was treated with the following, in order: toluene, isopropanol, water, piranha etch, water, chromic acid + sulfuric acid, and water. Following drying with a stream of nitrogen, the sensors were then further cleaned in an air plasma (Model PDC-3XG, Harrick Scientific, Ossining, NY) for 10 min.

Deposition was continued until the net frequency shift reached a value in the range of 130–260 kHz. Films of PIB, FPOL, PECH, OV-275, and PDPP were deposited successfully with this approach. Films of OV-25 were not — after deposition of only ~ 100 kHz, the sensor became unstable and then ceased to function. Microscopic examination of the films indicated that smooth, reasonably uniform films of the first five polymers were obtained, while that of OV-25 was a series of discrete beads, indicating poor wetting of the film to the silicon nitride surface of the sensor. Similar problems have been reported for this polymer on quartz SAW sensors [23]. The OV-275 film was also characterized by discrete coated domains separated by uncoated regions, but the wetting was better than that observed with the OV-25.

Pretreatment with saturated vapors of dimethyldichlorosilane following plasma cleaning did not improve adhesion of OV-25. Attempts to deposit an alterna-

tive coating, vinyl-terminated dimethyldiphenyl polysiloxane (OV-17, Supelco), which has structural features similar to OV-25, gave similarly poor results. The next replacement for OV-25 considered was a side-chain liquid crystalline polymer (SCLCP) containing alkylcyanobiphenyl side-chain moeities along a polyacrylate backbone whose structure and properties are described elsewhere [24]. It has exhibited good surface-wetting properties and long-term stability on quartz SAW sensors. The deposited film of this material was smooth and continuous.

The mass per unit area, m, of the coating film on each sensor was estimated from the frequency shift, Δf, using the following equation derived from an expression for the phase velocity of the 0th-order antisymmetric flexural plate mode [16,17]:

$$\Delta m = M\left\{\left[F_0/(F_0 - \Delta f)\right]^2 - 1\right\} \quad (1)$$

where F_0 is the initial sensor frequency and M the mass per unit area of the uncoated FPW membrane. A value of $M = 1.99$ mg/cm^2 was determined from the thicknesses and densities of the composite layers of the FPW membrane. Coating film thicknesses were then calculated using the polymer densities. The coating frequency shifts and calculated film thicknesses are as follows: SCLCP (130 kHz, 650 nm), FPOL (192 kHz, 580 nm), PDPP (206 kHz, 850 nm), PECH (254 kHz, 930 nm), OV-275 (136 kHz, 680 nm), and PIB (192 kHz, 1040 nm).

Shortly after coating, the sensor coated with OV-275 became unstable and failed temporarily, but recovered upon standing overnight and functioned normally for all subsequent testing. The PIB-coated sensor, however, failed and could not be resurrected. Thus, results reported below are for the remaining five sensors.

2.3. Calibration and testing

Table 1 lists the eight solvent vapors tested and the range of vapor concentrations over which the instrument was calibrated. Several aromatic and chlorinated solvents were included in the vapor set to explore capabilities for within-class discrimination. All solvents were obtained from Aldrich (Milwaukee, WI) at > 98% purity and were used as received.

Test atmospheres of the individual vapors or vapor mixtures were prepared by injecting a known volume of liquid solvent into a seasoned (i.e., pre-exposed and purged) 3-l Tedlar® bag and diluting with a known volume of clean, filtered air at 50% RH. In a typical exposure series, five bags were prepared, each at a given vapor concentration. After mixing by physical agitation, the bag was attached to the inlet valve of the instrument using a short section of narrow-bore Teflon® tubing. At the start of each calibration, a series of four or five samples of clean, filtered air at 50% RH was measured and the response maxima due to water vapor were averaged. Since the response peak for water vapor partially overlapped those of all of the solvent vapors at the higher flow rates employed during calibration and testing, a fraction of the peak response due to the blank for each sensor was subtracted from subsequent organic vapor response maxima. Typical water-vapor (blank) maxima values are given in Table 1. Three binary mixtures and three ternary mixtures of subsets of these vapors were also tested at different component concentrations. All test atmospheres were analyzed with a gas chromatograph (GC) (Model 5730; Hewlett Packard, Palo Alto, CA) equipped with a 2-ft 1/8-in. i.d., packed column (1% SP-1000 on 60/80 mesh Carbopack B; Supelco) and an FID. A gas-tight syringe was used to extract replicate aliquots of each test-atmosphere for analysis.

Linear regression analysis with forced zero provided calibration curves for each vapor-sensor pair over the range of concentrations examined. Pattern recognition was performed using extended disjoint principal component (EDPCR) analysis [1–3,25]. Monte Carlo simulations employed an error model described elsewhere [2,3], which

Table 1
Sensitivities and LODs for the test vapors[a]

Vapor	p_v^b	Concentration range[c]	Sensitivity[d] (LOD[c])				
			SCLCP	FPOL	PDPP	PECH	OV-275
Benzene (BEN)	92	50–600	8.8 (13)	43.9 (6.1)	123 (1.6)	163 (1.1)	28.9 (5.9)
Toluene (TOL)	27	40–210	21.5 (5.5)	76.8 (3.5)	151 (1.3)	252 (0.7)	43.1 (3.9)
m-Xylene (XYL)	9	36–200	45.3 (2.6)	144 (1.9)	246 (0.8)	421 (0.4)	74.5 (2.3)
Trichloroethylene (TCE)	65	50–250	8.5 (14)	24.8 (11)	55.6 (3.6)	64.1 (2.8)	14.1 (12)
Perchloroethylene (PCE)	18	40–250	23.2 (5.1)	77.0 (3.5)	218 (0.9)	182 (1.0)	52.5 (3.2)
2-Butanone (MEK)	100	50–400	10.8 (11)	467 (0.6)	102 (1.9)	260 (0.7)	43.9 (3.9)
n-Butylacetate (BAC)	27	50–400	25.2 (4.7)	880 (0.3)	132 (1.5)	477 (0.4)	63.6 (2.7)
2-Propanol (IPA)	42	50–450	1.6 (75)	58.5 (4.6)	9.0 (22)	20.6 (8.6)	10.5 (16)
Water[e]	24	15,800	0.011 (–)	0.079 (–)	0.010 (–)	0.042 (–)	0.035 (–)

[a] 34 ml/min, 60-s sample, RH = 50%.
[b] Vapor pressure in mm Hg at 25°C.
[c] In ppm.
[d] In Hz/ppm.
[e] 50% RH.

accounts for variations in sample volume, desorption heating rate, baseline noise, residual water vapor in desorbed samples, and calibration procedures. All of these factors were quantified experimentally.

3. Results and discussion

3.1. Response characteristics

Response profiles were highly reproducible among replicate exposures, with relative standard deviations of the maxima of four replicates at a given concentration typically ranging from 0.6% to 3.5%. The consistency of sequential response maxima indicates no significant residual carryover of vapor on the Tenax-GR adsorbent in the preconcentrator. This was also confirmed by a separate series of experiments.

Duplicate response profiles for 210 ppm of toluene from two representative sensors at a flow rate of 34 ml/min are presented in Fig. 3. They are typical of those observed for the other vapors tested. The symmetry of each profile reflects the relative vapor sorption/desorption kinetics in each polymer coating. All sensors gave apparent rise times (90%) of ~ 1 s for toluene. Recovery times (90%) for the PDPP, PECH and OV-275 sensors were ≤ 4 s, while those for the FPOL and SCLCP sensors were about 8 and 11 s, respectively. A small baseline shift was also consistently observed for the latter sensors. Slow diffusion of vapors into these polymers has been noted previously [24,26].

Peak widths (full-width at half maximum) of desorbed samples (at 200–270 ppm) collected for 60 s at 34 ml/min ranged from 0.85 s (for TCE on PDPP) to 3.6 s (for BAC on FPOL). This summary measure of the response profiles reflects a combination of the desorption rate from the preconcentrator, the system dead volume, and the rate of vapor partitioning into and out of the sensor coatings. The latter is affected by the affinity of the vapor for the coating — in general, those vapors giving smaller peak responses at a given vapor concentration also give narrower peaks,

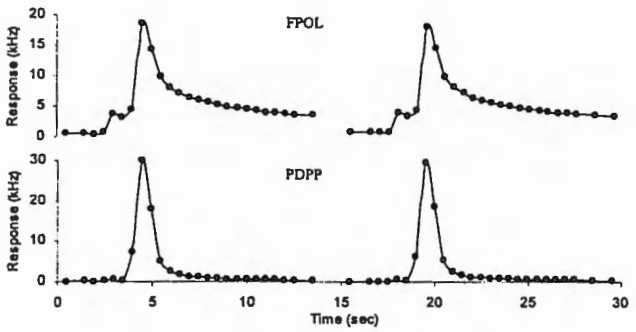

Fig. 3. Response profiles of the FPOL- and PDPP-coated sensors upon exposure to a thermally desorbed sample of toluene (200 ppm for 60 s) at 34 ml/min.

which suggests that mass transfer within the polymer films is an important variable (see below).

At this point, it became apparent that the data acquisition rate of the instrument was a limiting factor in defining the response profiles. Attempts to increase the rate were unsuccessful. As noted above, reproducible maxima and peak shapes are obtained despite this limitation, however, it is not clear whether the true maximum of each peak is captured in all cases.

Elution times, measured from the start of the desorption heat pulse to the response maximum, range from 2 to 4.5 s and vary inversely with the vapor pressure of the analyte and the flow rate. Water vapor elutes more rapidly than the test vapors (~ 1.5 s), consistent with our previous findings using a different hydrophobic adsorbent [2,3] and with the expectation of a weaker affinity of the adsorbent for water vapor.

3.2. Sensitivities and LODs

Table 1 shows the matrix of sensitivities and LODs for a 60-s sample at a flow rate (sampling and desorption) of 34 ml/min. Sensitivities for each vapor/sensor pair were determined from the slopes of the calibration curves. Coefficients of determination (r^2) were all ≥ 0.98. The sensitivities in Table 1 are averages of 2–4 calibrations with the exception of those for toluene, which are based on six calibrations. The relative standard deviation of the sensitivities were < 12% in all cases, and were typically < 6%.

The sensitivities are quite high compared to SAW sensors coated with the same polymers operated under similar conditions (i.e., with preconcentration) [2,3,11,27], owing to a combination of the relatively thick polymer layers employed, the efficiency of thermal desorption of preconcentrated samples, and the low dead volume of the sensor array. However, the baseline noise levels for these sensors, which typically ranged from 30 to 85 Hz (rms), are also quite high and the resulting LODs are greater than expected. The major source of baseline noise was found to be the instrument pump. With the pump off, baseline noise levels were reduced to 1–2 Hz (rms). Although the pump was mounted on a vibration dampening platform and a pulse dampener was inserted upstream, it is clear that improvements in either the mechanical isolation or pneumatic profile of the pump would lead to significant improvements in LODs.

If the LOD is defined as 3σ/sensitivity, where σ is the rms baseline noise, LOD values range from 0.3 ppm (*n*-butyl acetate on FPOL) to 4.6 ppm (isopropanol on FPOL) when based on the *most* sensitive sensor in the array, and generally increase with increasing solvent vapor pressure, as expected [22]. If the LOD is based on the *least* sensitive sensor in the array, the values increase to 2.6 ppm (*m*-xylene on SCLCP) and 75 ppm (isopropanol on SCLCP). This latter LOD is probably the more relevant measure of performance in the low concentration limit

since measurable signals from several sensors (if not all five sensors) are generally required for the purposes of vapor recognition. In fact, it has been shown that the ability to recognize a vapor from its response pattern often requires signals that are well above the LOD, even when the LOD is based on the least sensitive sensor in the array [27].

The six toluene calibrations performed over the 2-month testing period provide a measure of the stability of the instrument performance. The relative standard deviation of the slopes ranged from 1–6% among the five sensors with no trends observed over time.

3.3. Sample volume and flow rate effects

Increasing the sample volume (time) was explored as a means of increasing sensitivity and decreasing the LOD. Fig. 4a and b shows the results for toluene of increasing the sample volume at each of several flow rates for the FPOL- and PDPP-coated sensors, respectively. At a given flow rate the sensitivity initially increases in proportion to the sample time but eventually approaches a plateau indicating loss of sample due to breakthrough of the adsorbent in the preconcentrator. The time at which breakthrough is evident varies inversely with the flow rate (i.e., sample volume) as expected.

The difference in the apparent breakthrough time between the FPOL- and PDPP-coated sensors is noteworthy. The slower responding FPOL-coated sensor maintains its proportionality with the sample duration out to somewhat longer times than the faster responding PDPP-coated sensor. The SCLCP-coated sensor behavior tracked that of the FPOL-coated sensor and the remaining sensors tracked that of the PDPP-coated sensor. If the mass transfer rate is a limiting factor, then this might contribute to the non-linearity in the plots shown in Fig. 4, since the amount of vapor that must partition into and out of the coating films increases with the sample volume (time). If this were the case, however, we would expect the slower FPOL to show a greater effect. But, as shown in Table 1, the sensitivity of the PDPP-coated sensor to toluene is about twice that of the FPOL-coated sensor. Thus, although peak width measurements indicate that diffusion of toluene is faster in the PDPP, the fact that more vapor must be sorbed and

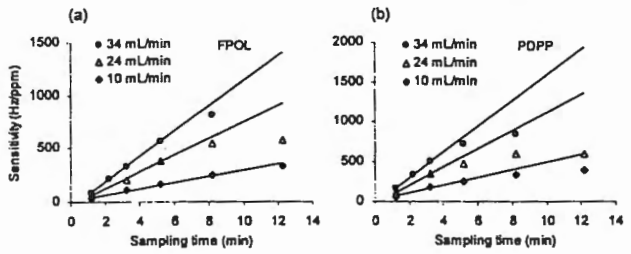

Fig. 4. Dependence of the sensor responses of the sample duration for different flow rates (toluene concentration = 85 ppm).

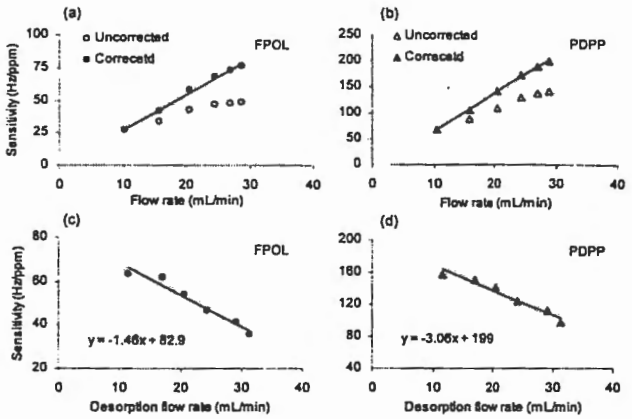

Fig. 5. Dependence of sensor responses on flow rate for (a) FPOL- and (b) PDPP-coated sensors. Uncorrected responses (open symbols) were measured directly. Corrected responses (filled symbols) account for the loss in sensitivity with increasing desorption flow rate as shown in (c) and (d).

desorbed by the PDPP than by the FPOL apparently accounts for the trends seen in Fig. 4. It is also possible that the slow data acquisition rate is contributing, since the ability to capture the response peak may also decline with increasing sample size. This would be more critical for the faster responding PDPP than for the FPOL.

Similar experiments run at higher vapor concentrations showed similar trends with shorter linear ranges. At flow rates > 10 ml/min and toluene concentrations > 300 ppm the sample time was constrained to < 3 min.

Increasing the flow rate at a given concentration and at a fixed sampling time of 60 s leads to an increase in response. The open symbols in Fig. 5a and b represent results, again for the FPOL- and PDPP-coated sensors, upon exposure to 85 ppm of toluene. Although the increase in response is roughly linear, the slopes of the curves are shallower than expected and give positive intercepts for all sensors.

An additional series of experiments was performed where the sample time and sampling flow rate were kept constant at 60 s and 24 ml/min, respectively, and the desorption flow rate was varied from 10 to 32 ml/min for a series of sequential trials. This required stopping the flow momentarily after sample collection so that the pump flow rate could be adjusted to the desired level prior to activating the heater for thermal desorption. Results are shown in Fig. 5c and d for FPOL and PDPP, respectively. As the desorption flow rate increases, the response maxima decrease proportionally, even though the elution times and peak widths also decrease (not shown). The pressure drop associated with the increase in desorption flow rate was very small over this range of flow rates and could not account for the decreases in response.

A set of correction factors was calculated by multiplying the slope from Fig. 5c or d (or similar plots for the other sensors) by the increase in the flow rate above 10

ml/min. Adding this correction factor to the measured responses (open symbols in Fig. 5a and b) gave the corrected values represented by the filled symbols in Fig. 5a and b. As shown, the responses become linear with flow rate and have zero y-intercepts.

As the flow rate is increased from 10 to 36 ml/min the sample residence time within each 3-μl sensor cell decreases from 108 to 30 ms. Assuming diffusional mass transport within the coating films, the Einstein equation for planar diffusion (i.e., $x^2 = 4Dt$) can provide a rough estimate of the time for diffusion into the coating films. For a film thickness (x) ranging from 0.6 to 1 μm and an assumed vapor diffusion coefficient (D) of 10^{-7} cm^2/s, the time (t) for a vapor molecule to diffuse through the polymer films ranges from about 9 to 25 ms. This indicates that diffusion times are of the same order as sample residence times above the sensors, and it is reasonable to conclude that sorption equilibrium is not necessarily being reached at the higher flow rates. That is, kinetic effects may indeed be influencing the responses observed.

3.4. Mixture responses

Previous work in our laboratory with polymer-coated SAW sensor arrays used in configurations similar to that used here with the FPW sensor array has revealed that responses to vapor mixtures are equivalent to the sum of the responses to the individual vapors at the same concentrations [1–3]. To determine whether this was the case for the current instrument a series of binary and ternary vapor mixtures was generated and analyzed. For each mixture, three test-atmospheres with different absolute and relative vapor concentrations were generated.

Expected responses were determined from the calibration data for the individual vapors: responses at the component concentrations derived from the individual-vapor calibration curves were added for all co-eluting or partially overlapping mixture components and then compared to the actual (experimental) mixture responses. As shown in Table 2, average deviations from additivity ranged from positive to negative and were all $< 10\%$. The largest individual deviation observed was 14% (for the OV-275-coated sensor response to one of the PCE + TOL exposures), but this was exceptional. No systematic trends were observed. Thus, within experimental error, the additivity assumption appears valid. This is a key factor in the EDPCR methodology [25].

Table 2
Deviation of the mixture response from the sum of component responses for several binary and ternary vapor mixtures

Vapor mixture	Relative deviation (%)[a]				
	SCLCP	FPOL	PDPP	PECH	OV-275
BAC+MEK	5.5	5.4	−2.7	4.1	6.0
PCE+TOL	−2.0	7.0	−5.2	7.4	−5.5
XYL+IPA	1.0	−3.5	−6.1	−0.5	1.1
BEN+BAC+MEK	0.7	−2.6	1.3	4.4	−1.4
BEN+XYL+IPA	0.8	1.8	4.2	2.2	6.1
BAC+PCE+TOL	−1.0	7.8	−1.1	7.3	9.5

[a] Each value is the average from three exposures at different absolute and relative concentrations.

Elution times were not affected by the presence of other vapors in the preconcentrated samples and most vapors co-eluted from the preconcentrator. Peaks from vapors differing significantly in vapor pressure (e.g., m-xylene and isopropanol) were partially separated. It was noted that as the desorption flow rate was increased these peaks tended to coalesce.

3.5. Vapor recognition

Response patterns constructed from the sensitivity values in Table 1 revealed the expected similarities among the aromatic and chlorinated hydrocarbon vapors. The patterns for MEK and BAC were also similar. In all cases, however, there were subtle differences in the response patterns. The data were analyzed by EDPCR to establish a training set of response patterns corresponding to each vapor. For mixtures, the assumption of additivity was made to allow construction of a training set of composite response patterns for all possible mixtures at all possible relative concentrations. The concentrations of the mixture components could be determined by decomposing the composite patterns as described elsewhere [1,25].

Two approaches were used to test the ability of the array to recognize and discriminate among the different vapors. First, an independent test set was generated for seven of the eight individual vapors at two or more different concentrations. Response patterns from this test set were compared to those from the training set via EDPCR to determine the identity and concentration of each vapor. A similar approach was used to analyze the response data used to generate Table 2, except that these mixture response data were combined with a subset of the individual-vapor data and the capability for the array to discriminate among the components of each of the 3-vapor subsets was evaluated.

The second approach to assessing array performance involved the use of Monte Carlo simulations in conjunction with EDPCR. Using the calibrated sensitivities from Table 1, an initial (synthetic) response value was calculated from a randomly selected concentration within the calibrated range. Error was then added to this response using a model described elsewhere [3]. The error model employed accounts for all known sources of response variation in the instrument. Error-enhanced synthetic responses were generated iteratively and each was treated as an unknown that was then assigned an identity by comparison (via EDPCR) with the response patterns established from the calibration data. The number and nature of recog-

nition errors observed from a large sample set (i.e., hundreds of simulations) were logged and evaluated. Similar procedures were used for the analysis of mixtures of 2–5 vapors.

3.6. Independent test sets

Results of the analysis of the first independent test set are summarized in Table 3. Each individual test-vapor response pattern was compared to the response patterns of the eight vapors. If it was correctly recognized, then its concentration was estimated. As shown in Table 3, the only two recognition errors occurring out of the 23 cases entailed confusion of PCE for TCE and benzene for toluene. The overall rate of correct recognition was, therefore, 91.3% (21/23). Errors in quantification ranged from 0.1 to 18% and averaged 5%.

For the mixtures the recognition problems were formulated differently. Each of three 3-vapor subsets was considered separately and the simulations were performed to assess whether all three possible individual vapors, one of the binary mixtures, and the ternary mixture could be recognized and differentiated from each other. Only one of the three possible binary mixtures was tested and only a few exposures to each test vapor or test mixture were performed.

Table 3
Individual test-vapor recognition and quantification results (independent test set)

Vapor	Recognized as	Concentration (ppm)		% Error
		Actual	Measured	
BEN	BEN	200	204	1.9
	BEN	200	191	−4.5
TOL	TOL	101	102	1.0
	TOL	151	153	1.3
	BEN	54	75	–
XYL	XYL	146	154	5.5
	XYL	256	263	2.7
	XYL	366	365	−0.3
PCE	PCE	146	155	6.2
	PCE	98	97	−1.0
	TCE	49	147	–
MEK	MEK	200	164	−18
	MEK	300	286	−4.7
	MEK	400	393	−1.8
BAC	BAC	191	205	7.3
	BAC	286	316	10
	BAC	394	405	2.8
	BAC	68	57	−13
	BAC	136	131	−3.7
	BAC	204	197	−3.4
IPA	IPA	230	212	−7.8
	IPA	341	326	−3.5
	IPA	427	426	−0.2
Recognition rate	91.3%			
Average quantification error				5.0%

For the subset consisting of toluene, PCE and *n*-butyl acetate, performance was extremely good, with 14 of the 15 tests resulting in a correct recognition. The only error was confusion of toluene as a mixture of toluene with a low concentration of PCE. For the subset consisting of *n*-butyl acetate, MEK, and benzene, the performance was quite poor, with only five of the thirteen exposures resulting in a correct recognition. Although the *n*-butyl acetate was consistently recognized correctly, there were several errors in recognizing MEK and benzene. The last 3-vapor subset considered was *m*-xylene, benzene, and isopropanol. In this case, again, very poor results were obtained — only 3 of the 13 exposures resulted in correct recognition, and these were all for isopropanol alone. Neither *m*-xylene nor benzene as individual vapors, or any of the mixtures containing these two vapors were correctly recognized in this subset.

3.7. EDPCR / Monte Carlo analyses

The first case considered using the EDPCR/Monte Carlo approach was where the responses to an individual vapor had to be recognized as one of the eight possible vapors in the training set (no mixtures were considered). The procedure of generating synthetic responses and assigning identities was performed 500 times for each of the eight vapors (i.e., 4000 simulations) to obtain a stable statistical estimate of the reliability of recognition. The allowed concentration range was 3–30 × LOD, where the LOD was defined as that corresponding to the least sensitive sensor in the array for the specific vapor under consideration.

The predicted average recognition rate was 98.7%. The only significant confusion predicted was between toluene and *m*-xylene. A low level of confusion was also predicted between toluene and benzene. No other recognition errors were expected on the basis of the Monte Carlo simulations. Overall, the predicted results agree quite well with those obtained experimentally from the independent test set of individual vapors (notwithstanding the one case of confusion of PCE with TCE, which was observed experimentally but not predicted).

The next series of simulations considered the 3-vapor subsets analyzed experimentally. Predicted rates of recognition, based on weighted averages that accounted for which of the specific vapors and mixtures were actually tested, were 87%, 65%, and 81%, respectively. The high rate predicted for the first subset agrees well with the experimental results. Although the recognition rates predicted for the next two subsets were lower than the first, as observed experimentally with the independent test sets, the recognition rates predicted are much higher than those achieved experimentally.

Part of this discrepancy can be attributed to the limited number of experimental tests performed, but the quantitative agreement between experimental and simulated recog-

Table 4
Average vapor recognition rates for multi-vapor subsets predicted by EDPCR/Monte Carlo analysis

No. of vapors	Vapor subset	Recognition rate (%)	No. of vapors	Vapor subset	Recognition rate (%)
2	BEN + IPA	99.6	3	TOL + PCE + IPA	92.9
	PCE + BAC	98.9		IPA + PCE + MEK	92.2
	TCE + IPA	98.4		BEN + MEK + IPA	92.1
	MEK + TOL	97.2		XYL + PCE + BAC	88.6
	XYL + MEK	95.5		TOL + PCE + MEK	87.0
	BEN + XYL	85.9		BEN + BAC + PCE	86.0
	TCE + PCE	85.6		MEK + BAC + IPA	76.1
	MEK + BAC	83.1		TOL + XYL + TCE	59.5
	TOL + XYL	72.4		TOL + BEN + XYL	52.7
4	TOL + PCE + BAC + IPA	83.4	5	XYL + BEN + PCE + BAC + IPA	69.6
	XYL + PCE + MEK + IPA	79.2		TOL + BEN + PCE + MEK + IPA	66.1
	TCE + PCE + MEK + IPA	67.4		MEK + BAC + IPA + BEN + PCE	52.4
	BEN + TOL + XYL + TCE	42.2		BEN + TOL + XYL + TCE + PCE	28.9

nition rates is not very good. At the same time, the nature of the errors was predicted by the Monte Carlo simulations quite well. That is, for the second 3-vapor subset, the highest rate of error was predicted to occur with the ternary mixture, which was observed. For the third 3-vapor subset, low errors were predicted for isopropanol alone and greater errors were predicted for the mixtures, both of which were also observed.

To explore the performance of the instrument for mixture analyses more generally, several additional series of simulations were performed. Subsets of two, three, four, and five vapors were selected from the eight vapors on the basis of cluster analyses to span the range of difficulty in recognition expected for the data set. As above, these mixture analyses considered the recognition and discrimination of all possible sub-components of a vapor subset of a given size. For subsets of two, three, four, and five vapors, the number of possible sub-components that must be discriminated is 3, 7, 15, and 31, respectively.

Results are summarized in Table 4 as the average recognition rates obtained for representative vapor subsets. Recognition rates range from 72% to 97% for the subsets of two vapors, and show the expected decrease in recognition for subsets comprising vapors from the same chemical class (e.g., toluene and *m*-xylene). For the subsets of three vapors, recognition rates range from 53% to 93% and show the same trends with subset composition as for the 2-vapor subsets. Errors in recognition become very high where subsets of four or more vapors are considered indicating that reliable performance would not be possible for any of these cases.

4. Conclusions

This preliminary investigation of an instrument employing an integrated array of polymer-coated FPW sensors has shown the capability for rapid, effective multi-vapor analysis. Instrument performance benefits from the stable responses provided by the array, the efficiency of the preconcentrator in trapping and subsequently thermally desorbing sampled vapors, and the low-dead volume of the system. Sub-ppm LODs are achievable for many vapors with a 60-s sampling time, and reductions in the LODs by an order of magnitude are expected for all analytes by better vibration isolation and pneumatic dampening of the sampling pump in the instrument.

Our probe of the sampling and desorption flow rate effects revealed the possibility for kinetic factors, related to vapor sorption in the sensor coatings, limiting the responses. However, the relatively slow data acquisition rate of the instrument software precludes a definitive conclusion about this issue. Increases in the instrument data acquisition rate are clearly needed to better define response peaks.

Unique response patterns were obtained for the eight vapors tested, and each could be recognized and differentiated from the others in the test set with very low error. Mixtures could also be analyzed with low error in certain cases. Exceptions were mixtures containing homologous or otherwise similar vapors. Difficulty was encountered in analyzing mixtures of four or more vapors, as has been reported previously using an array of similarly coated SAW sensors [3], suggesting that arrays of polymer-coated acoustic-wave sensors may be limited to the analysis of relatively simple mixtures of structurally heterogeneous vapors.

Acknowledgements

The authors are indebted to Stuart Wenzel, Ben Costello, and Eric Snyder of Berkeley MicroInstruments, for technical assistance and valuable discussions, and to Art Snow for providing a sample of FPOL. Funding was provided by

Grant R01-OH03692 from the National Institute for Occupational Safety and Health of the Centers for Disease Control and Prevention (NIOSH-CDCP) and by a subcontract from Berkeley MicroInstruments, (U.S. Air Force SBIR Grant F0865-93-C-0096).

References

[1] E.T. Zellers, S. Batterman, M. Han, S.J. Patrash, Optimal coating selection for the analysis of organic vapor mixtures with polymer-coated surface acoustic wave sensor arrays, Anal. Chem. 67 (1995) 1092–1106.

[2] J. Park, G.-Z. Zhang, E.T. Zellers, Personal monitoring instrument for the selective measurement of multiple organic vapors, Am. Ind. Hyg. Assoc. J. (2000) in press.

[3] J. Park, W.A. Groves, E.T. Zellers, Vapor recognition with small arrays of polymer-coated microsensors — a comprehensive analysis, Anal. Chem. 71 (1999) 3877–3886.

[4] D.S. Ballantine, R.M. White, S.J. Martin, A.J. Ricco, G.C. Frye, E.T. Zellers, H. Wohltjen, Acoustic Wave Sensors: Theory, Design, and Physicochemical Applications, Academic Press, Boston, MA, 1997.

[5] A.J. Ricco, R.M. Crooks, G.C. Osbourne, Surface acoustic wave chemical sensor arrays: new chemically sensitive interfaces combined with novel cluster analysis to detect volatile organic compounds and mixtures, Acc. Chem. Res. 31 (1998) 289–296.

[6] M.C. Lonergan, E.J. Severin, B.J. Doleman, S.A. Beaber, R.H. Grubbs, N.S. Lewis, Array-based vapor sensing using chemically sensitive carbon black-polymer resistors, Chem. Mater. 8 (1996) 2298–2312.

[7] W.P. Carey, K. Beebe, B.R. Kowalski, Multicomponent analysis using an array of piezoelectric crystal sensors, Anal. Chem. 59 (1987) 1529–1534.

[8] A. Hierlemann, U. Weimar, G. Kraus, G. Gauglitz, Environmental chemical sensing using quartz microbalance sensor arrays: application of multicomponent analysis techniques, Sens. Mater. 7 (1995) 179–189.

[9] T.A. Dickinson, D.R. Walt, J. White, J.S. Kauer, Generating sensor diversity through combinatorial polymer synthesis, Anal. Chem. 69 (1997) 3413–3418.

[10] J.R. Stetter, P.C. Jurs, S.L. Rose, Detection of hazardous gases and vapors: pattern recognition analysis of data from an electrochemical sensor array, Anal. Chem. 58 (1986) 860–866.

[11] W.A. Groves, E.T. Zellers, G.C. Frye, Analyzing organic vapors in exhaled breath using a surface acoustic wave sensor array with preconcentration: selection and characterization of the preconcentrator adsorbent, Anal. Chim. Acta 371 (2/3) (1998) 131–143.

[12] J.W. Grate, S.L. Rose-Pehrsson, D.L. Venezky, M. Klusty, H. Wohltjen, Smart sensor system for trace organophosphorus and organosulfur vapor detection employing acoustic wave sensors, automated sample preconcentration, and pattern recognition, Anal. Chem. 65 (1993) 1868–1881.

[13] R.M. White, P.J. Wicher, S.W. Wenzel, E.T. Zellers, Plate-mode ultrasonic oscillator sensors, IEEE Trans. Ultrason., Ferroelectr., Freq. Control 34 (1987) 162–177.

[14] E.T. Zellers, R.M. White, S.W. Wenzel, Computer modeling of polymer-coated ZnO/Si surface-acoustic-wave and lamb-wave chemical sensors, Sens. Actuators 14 (1988) 35–45.

[15] S.W. Wenzel, R.M. White, Flexural plate-wave gravimetric chemical sensor, Sens. Actuators, A 21/23 (1990) 700–703.

[16] S.W. Wenzel, R.M. White, Flexural plate-wave sensor: chemical vapor sensing and electrostrictive excitation, Proc. IEEE Ultrasonics Symposium, Montreal, October 3–6, 1989.

[17] J.W. Grate, S.W. Wenzel, R.M. White, Flexural plate wave devices for chemical analysis, Anal. Chem. 63 (1991) 1552–1561.

[18] S.W. Wenzel, R.M. White, A multisensor employing an ultrasonic Lamb-wave oscillator, IEEE Trans. Electron Dev., Special Issue on Microsensors and Microactuators, Vol. ED-35, June 1988, pp. 735–743.

[19] G.C. Frye-Mason, R.J. Kottenstette, E.J. Heller, C.M. Matzke, S.A. Casalnuovo, P.R. Lewis, R.P. Manginell, W.K. Schubert, V.M. Hietala, R.J. Shul, Integrated chemical analysis systems for gas phase CW agent detection, in: D.J. Harrison, A. van den Berg (Eds.), Proc. Micro Total Analysis Systems '98 (μTAS '98), Kluwer Academic Pub., Boston, 1998, pp. 477–481.

[20] J.W. Grate, M. Abraham, Solubility interactions and the design of chemically selective sorbent coatings for chemical sensors and arrays, Sens. Actuators, B 3 (2) (1991) 85–111.

[21] J.W. Grate, G.C. Frye, Acoustic wave sensors, in: H. Baltes, W. Gopel, J. Hesse, (Eds.), Sensors Update, Chap. 2, Vol. 2, VCH, Weinheim, FRG, 1996, pp. 37–83.

[22] S.J. Patrash, E.T. Zellers, Characterization of polymeric surface-acoustic-wave sensor coatings and semi-empirical models of sensor responses to organic vapors, Anal. Chem. 65 (1993) 2055–2066.

[23] J.W. Grate, A.R. McGill, Dewetting effects on polymer-coated surface-acoustic-wave vapor sensors, Anal. Chem. 67 (1995) 4015–4019.

[24] E.T. Zellers, M. Oborny, R. Thomas, A. Ricco, G.C. Frye-Mason, G.-Z. Zhang, C. Pugh, Shape-selectivity with liquid crystal and side-chain liquid crystalline polymer SAW sensor interfaces, Proceedings of the Eurosensors 13th Conference, The Hague, The Netherlands, September 12–15, 1999, pp. 73–74.

[25] E.T. Zellers, T.S. Pan, S. Patrash, M. Han, S. Batterman, Extended disjoint principal components regression analysis of SAW vapor sensor array responses, Sens. Actuators, B 12 (2) (1993) 123–133.

[26] J.W. Grate, S.J. Patrash, S.N. Kaganove, B.M. Wise, Hydrogen bond acidic polymers for surface acoustic wave vapor sensors and arrays, Anal. Chem. 71 (1999) 1033–1040.

[27] E.T. Zellers, J. Park, T. Hsu, W.A. Groves, Establishing a limit of recognition for a vapor sensor array, Anal. Chem. 70 (1998) 4191–4201.